



HYBRID METAL-POLYMER NANOCOMPOSITES BASED ON POLYPHENOXAZINE AND COBALT NANOPARTICLES

Galina Petrovna Karpacheva,^{[a]*} Sveta Zhiraslanovna Ozkan,^[a] Ella Leont'evna Dzidziguri,^[b] Petr Aleksandrovich Chernavskii,^[c] Igor Sergeevich Eremeev,^[a] Mikhail Nikolaevich Efimov,^[a] Mikhail Ivanovich Ivantsov,^[c] and Galina Nikolaevna Bondarenko^[a]

Keywords: polymers with a polyconjugated system; polyphenoxazine; IR heating; Co nanoparticles; metal-polymer nanocomposite; hybrid magnetic nanomaterial.

It was shown for the first time, that after IR heating of polyphenoxazine in the presence of cobalt(II) acetate $\text{Co}(\text{CH}_3\text{CO}_2)_2 \cdot 4\text{H}_2\text{O}$ in the inert atmosphere at the temperature of 450–650 °C, the growth of the polymer chain via the condensation reaction of phenoxazine oligomers happens simultaneously with the dehydrogenation of phenyleneamine structures with the formation of conjugated C=N bonds. Hydrogen emitted during these processes contributes to the reduction of Co^{2+} to Co^0 . As a result the nanostructured composite material in which Co nanoparticles are dispersed into the polymer matrix is formed. According to TEM Co nanoparticles have size $4 < d < 14$ nm. The investigation of magnetic and thermal properties of Co/polyphenoxazine nanocomposite has shown that the obtained nanomaterial is superparamagnetic and thermally stable.

* Corresponding Author

Tel: +74959554255

E-Mail: gpk@ips.ac.ru

- [a] A.V. Topchiev Institute of Petrochemical Synthesis, Russian Academy of Sciences, 29 Leninsky prospect, Moscow, 119991 Russia
- [b] National University of Science and Technology "MISIS", 4 Leninsky prospect, Moscow 119049 Russia
- [c] Department of Chemistry Lomonosov Moscow State University, 1-3 Leninskie Gory, Moscow 119991 Russia

Introduction

Hybrid polymer nanomaterials take a special place among advanced materials due to a set of physical-chemical properties.^{1–4} Hybrid nanomaterials, including polymers with a polyconjugated system, are able to show excellent electric, magnetic and electrochemical properties. This fact makes them promising systems for magnetic information recording, organic electronics, medicine, protection against electromagnetic radiation, contrasting materials for magnetic resonance tomography, microelectromechanic systems, rechargeable batteries, sensors and biosensors, supercapacitors, electrocatalysts, solar cells, displays and other electrochemical devices

In view of this, the exploring approaches to synthesis of new hybrid magnetic nanomaterials based on polymers with a polyconjugated system and high dispersed magnetic nanoparticles and systematic investigation of the structure, morphology and physical-chemical properties of the obtained nanomaterials, depending on the synthesis conditions, are important in both fundamental and applied aspects.

There are few reports related to 2004–2013 years, concerning magnetic nanocomposites, in which magnetic nanoparticles are dispersed in the polymer matrix. Generally, polyaniline (PANI) is applied as a polymer component. PANI takes a special place among the conducting polymers due to the ease of synthesis and doping/dedoping processes, stability of properties.

$\text{Fe}_3\text{O}_4/\text{PAN}$ nanocomposites were obtained via polymerization of aniline in presence of Fe_3O_4 nanoparticles using H_2O_2 as an oxidant.⁵ The nanocomposites were ferromagnetic, saturation magnetization $M_S = 6.2$ emu g^{-1} .

Nanocomposites based on PANI and Fe_3O_4 nanoparticles were obtained via polymerization of aniline in the mixture of solutions of iron(II) and iron(III) chlorides.^{6,7} There was a simultaneous growth of the polymer chain of PANI and synthesis of magnetite nanoparticles. The conductivity of the nanocomposite was $\sim 10^{-4}$ S cm^{-1} . Saturation magnetization $M_S = 48.4$ – 80.4 emu g^{-1} .

In situ oxidative polymerization of aniline in neutral medium in the presence of Fe_3O_4 nanoparticles applying ammonium persulfate as an oxidant with ultrasonic treatment allows to synthesize PANI nanocomposites with homogeneously dispersed Fe_3O_4 nanoparticles.⁸ Fe_3O_4 nanoparticles obtained via coprecipitation of iron(II) and iron(III) salts in aqueous solution of polyvinylpyrrolidone under ultrasonic stirring. The diameter of nanoparticles was ~ 10 nm. The conductivity σ decreased (from 6.4×10^{-2} to 7.0×10^{-4} S cm^{-1}) and the saturation magnetization M_S increased (from 0.06 to 30.6 emu g^{-1}) as Fe_3O_4 content increased (from 7 to 60 %).

The nanostructured material based on PANI and hematite nanoparticles, possessing electrical and magnetic properties at room temperature, was obtained in presence of naphthalenesulphonic acid as a dopant.⁹ Depending on synthesis conditions, PANI nanotubes or nanorods about 80–100 nm in diameter, containing Fe₃O₄ nanoparticles ($d \sim 10$ nm), can be obtained. When the content of Fe₃O₄ was 20 wt. % the conductivity of the material was $\sigma = 10^{-2}$ S cm⁻¹, saturation magnetization $M_S = 6$ emu g⁻¹.

Nanocomposites which represent PANI nanorods 600 nm in length and 80 nm in diameter with attached magnetite nanoparticles, were synthesized by self-assembly method in presence of dodecylbenzenesulfonic acid serving as a dopant and a surfactant. The obtained nanocomposites were thermally stable and were superparamagnetics.¹⁰ γ -Fe₂O₃/PANI nanocomposites, synthesized by the reverse micelle technique in the system toluene/Na-dodecylsulfate/water, also possessed superparamagnetic properties.¹¹

Nanocomposites based on sulfonated PANI were synthesized using Fe₃O₄ nanoparticles via oxidative copolymerization of aniline and 2,5-diaminebenzenesulfonic acid or 2-aminebenzenesulfonic acid.¹² The nanocomposites showed ferromagnetic behaviour at room temperature. The saturation magnetization $M_S = 0.98$ and 0.29 emu g⁻¹, the residual magnetization $M_R = 0.37$ and 0.06 emu g⁻¹ for nanocomposites based on 2-amine- and 2,5-diaminebenzenesulfonic acid, respectively. The presence of Fe₃O₄ nanoparticles embedded into the polymer matrix made the structure more ordered. The authors of this article also obtained nanocomposites of sulfonated PANI via oxidative copolymerization of aniline and 5-amine-2-naphthalene or 1-amine-5-naphthalenesulfonic acid in presence of Fe₃O₄ nanoparticles.¹³ The presence of negatively charged ion substituents increased the stability of the polymer due to the effect of selfdoping. Diameter of magnetite nanoparticles was 10–15 nm. The nanocomposites were ferromagnetic at room temperature as in [12]. However, the saturation magnetization was sufficiently higher $M_S = 9.7$ emu g⁻¹. The conductivity of the nanocomposite $\sigma \sim 0.5$ S cm⁻¹ was higher than the conductivity of PANI $\sigma \sim 10^{-3}$ S cm⁻¹.

The nanocomposite based on nanocrystalline α -Fe particles 10–25 nm in diameter regularly dispersed in the PANI matrix was obtained by milling the mixture of PANI and 10 wt. % of α -Fe nanoparticles 30 nm in diameter during 20 hours in a ball mill under cryogenic conditions at $T = -150$ °C.¹⁴ In that case a large amount of single domain α -Fe particles were formed that led to an increase of the coercive force H_C from 36 to 206 Oe. The critical size of the transition to the single-domain state for α -Fe was 12–15 nm.¹⁵⁻¹⁷

Earlier we obtained nanocomposites based on polydiphenylamine and Co nanoparticles via thermal transformations of the polymer in the presence of cobalt(II) acetate under IR heating.¹⁸⁻²⁰ Magnetic nanoparticles had size $2 < d < 8$ nm, which provided single-domain criteria. The squareness coefficient of the hysteresis loop $k_S = 0.08$ – 0.016 , indicating of a significant content of superparamagnetic cobalt particles. After a short-time oxidation of the nanocomposite in the air flow at the temperature of 412 °C there was a significant decrease of

saturation magnetization M_S , together with the decrease of the coercive force H_C and the residual magnetization M_R . It can be supposed that a part of Co nanoparticles oxidized completely and a part of the largest particles contained the non-oxidized Co under the oxide shell, and the size of the core was close to the critical superparamagnetic size. It was shown that Co/polydiphenylamine nanocomposite had a high thermal stability. In the inert atmosphere at 900 °C the residue was 79 %.

The mentioned short review indicates that nowadays the scientific literature does not possess any data about the systematic investigations of fundamental dependence of magnetic characteristics of metal-polymer nanocomposites based on polyconjugated polymer systems on the content of the nanomaterial, metal nanoparticles size, the polymer component structure, etc. There is also no information about the effect of the polyconjugated system and the interaction of metal and polymer components on magnetic properties.

In this work a new one-step method of synthesis of hybrid metal-polymer nanocomposite based on Co nanoparticles and polyphenoxazine (PPOA) – a thermally stable heterocyclic polymer with a polyconjugated system, an aromatic derivative of PANI, is described for the first time. The results of the study of the nanocomposite formation process via chemical transformations of PPOA in the presence Co(II) acetate Co(CH₃CO₂)₂·4H₂O under IR heating in the Ar atmosphere at 450–650 °C are shown. Magnetic and thermal properties of the obtained nanomaterials were studied.

Experimental

The monomer and reagents were prepared according to methods described in the paper.²¹ PPOA was obtained via interface oxidative polymerization ($[\text{monomer}] = 0.2$ mol L⁻¹, $[(\text{NH}_4)_2\text{S}_2\text{O}_8] : [\text{monomer}] = 1.25$).²¹ Ammonium persulfate (NH₄)₂S₂O₈ (analytical grade) was purified via recrystallization. Phenoxazine (Acros Organics, 99 %), isopropyl alcohol (high-purity grade), toluene (analytical grade), DMF (Acros Organics, 99 %) and Co(CH₃CO₂)₂·4H₂O (reagent grade) were used as received. Aqueous solutions of reagents were prepared using distilled water.

For the synthesis of Co/PPOA nanocomposite a common solution of PPOA and Co(CH₃CO₂)₂·4H₂O in DMF was prepared. Concentration of PPOA in DMF was 2 wt. %, content of cobalt [Co] was 5–30 wt. % relative to the weight of the polymer without the acid residue. After the solvent removal at $T = 85$ °C the precursor, consisting of PPOA and cobalt(II) acetate, was treated by IR radiation in the Ar atmosphere at $T = 450$ – 650 °C for 2–30 minutes via the use of the automatic device for IR heating²².

IR spectra of PPOA and Co/PPOA nanocomposites were recorded on an IFS 66v FTIR spectrometer in the range 4000–400 cm⁻¹. The samples were prepared as KBr pellets.

X-ray investigations of PPOA and Co/PPOA nanocomposite were performed at room temperature on a DIFREY-401 diffractometer (Russia) (CrK α radiation, Bragg–Brentano focusing).

Microphotographs of Co/PPOA nanocomposite were taken on a LEO912 AB OMEGA transmission electronic microscope.

The metal content in Co/PPOA nanocomposite was determined quantitatively by the atom-absorption spectrometry method on an AAS 30 spectrophotometer (Carl Zeiss JENA). The accuracy of the determination of Fe was $\pm 1.0\%$.

Magnetic characteristics of Co/PPOA nanocomposite were investigated on a vibrational magnetometer²³ at room temperature. The absolute magnetic moment value was determined using a cobalt standard with a mass of 2 mg.

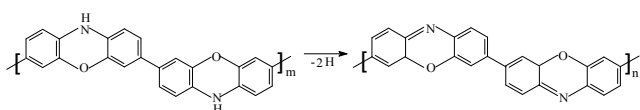
Thermal analysis of PPOA and Co/PPOA nanocomposite was carried out on a TGA/DSC1 device (Mettler Toledo) in dynamic regime in the range 30–1000 °C in air and in the flow of nitrogen. The loading of polymers was 100 mg, heating rate 10 °C min⁻¹, and the flow of nitrogen was 10 mL min⁻¹. Calcined alumina was used as a standard. The analysis of samples was conducted in Al₂O₃ crucibles.

DSC analysis was performed on a DSC823° calorimeter (Mettler Toledo). The samples were heated at a rate of 10 °C min⁻¹ in Ar flow of 70 mL min⁻¹. The measurement results were processed using STARE software supplied with the device.

Results and discussion

The synthesis of the hybrid metal-polymer nanocomposites based on PPOA and Co nanoparticles was carried out via chemical transformations of PPOA in the presence of cobalt(II) acetate Co(CH₃CO₂)₂·4H₂O in the inert atmosphere under IR heating. PPOA is a half-ladder heterocyclic polymer, containing both nitrogen and oxygen atoms, which are included into the whole system of polyconjugation. The molecular mass of PPOA is $M_w = 3.7 \times 10^4$. The choice of the polymer is defined by its high thermal stability (up to 400 °C in air and in the inert atmosphere at 1000 °C the residue is 51 %).²¹ The applying of IR radiation for chemical and structural modifications instead of the generally used thermal treatment is caused by the fact that due to the transition of the system into the vibrationally excited state it becomes possible to increase the rate of chemical reactions and to reduce the process time significantly.^{18-20,24,25}

During the IR heating of PPOA in the presence of cobalt(II) acetate Co(CH₃CO₂)₂·4H₂O the growth of the polymer chain occurs simultaneously with the dehydrogenation of phenyleneamine structures (B–NH–B) followed by the formation of conjugated C=N bonds.



It was found that during the IR heating in the presence of cobalt(II) acetate the growth of the polymer chain proceeds via the condensation reaction of phenoxazine oligomers.

Content of the oligomers in PPOA was proved by TGA and DSC.²¹ On the TGA curve a weight loss at 230 °C is observed, it is associated with the decomposition of the low-molecular fraction contained in the polymer. There is also an endothermic peak on the DSC image of PPOA at 285 °C associated with the decomposition.

According to IR spectroscopy data the growth of the polymer chain is proved by the intensity decrease of absorption band at 739 cm⁻¹, corresponding to nonplanar deformation vibrations of δ_{C-H} bonds of 1,2-substituted benzene ring of the end groups, i.e. the number of polymer end groups significantly reduces. Absorption bands at 869 and 836 cm⁻¹ are caused by nonplanar deformation vibrations of δ_{C-H} bonds of 1,2,4-substituted benzene ring (Figure 1). Presence of these bands indicates that the growth of the polymer chain proceeds via C–C - joining into *para*-position of phenyl rings with respect to nitrogen.²¹

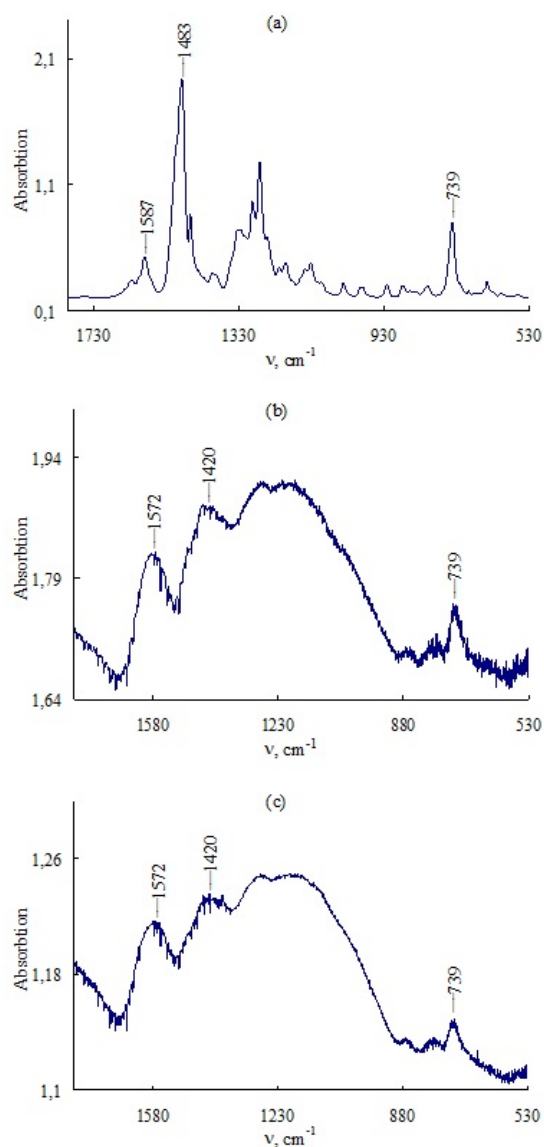


Figure 1. IR spectra of PPOA (a) and Co/PPOA nanocomposite, obtained at $T = 450$ (b) and 500 °C (c) while heating for 10 min in the region of absorption of nonplanar deformation vibrations of δ_{C-H} bonds of aromatic rings.

The formation of C=N bonds is proved by the shift and broadening of the bands at 1587 and 1483 cm^{-1} , corresponding to stretching vibrations of $\nu_{\text{C-C}}$ bonds in aromatic rings (Figure 1). Absorption band at 3380 cm^{-1} , corresponding to the stretching vibrations of $\nu_{\text{N-H}}$ bonds in phenyleneamine structures almost disappears. Absorption band at 3055 cm^{-1} in the PPOA IR spectrum corresponds to the stretching vibrations of the aromatic ring $\nu_{\text{C-H}}$ bonds. The absorption band at 3420 cm^{-1} , associated with water, appears (Figure 2).

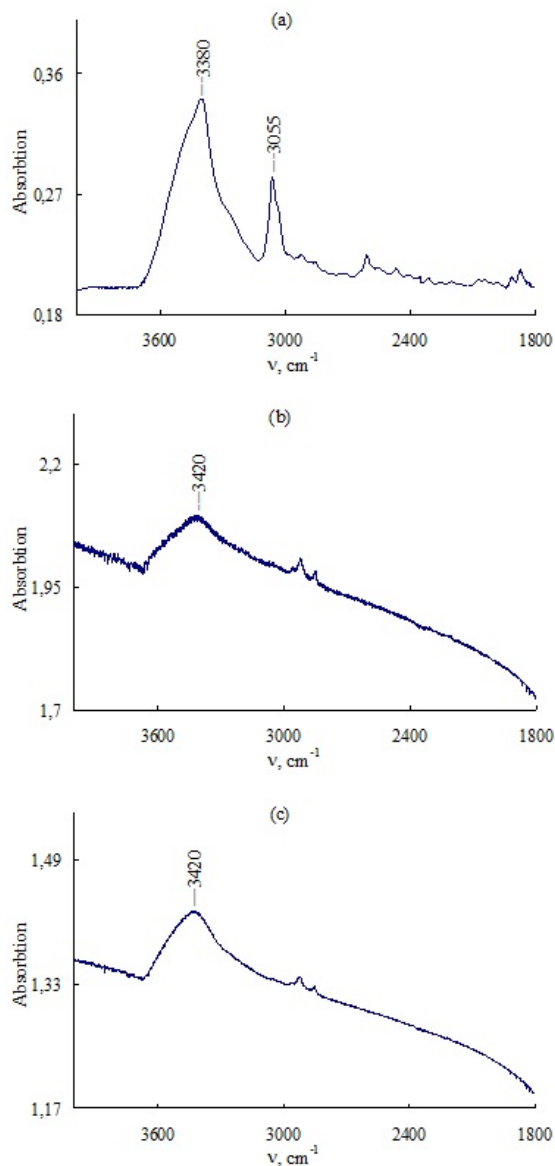


Figure 2. IR spectra of PPOA (a) and Co/PPOA nanocomposite, obtained at $T = 450$ (b) and 500 °C (c) while heating for 10 min in the region of absorption of stretching vibrations of $\nu_{\text{N-H}}$ and $\nu_{\text{C-H}}$ bonds.

Hydrogen released during these processes contributes to the reduction of Co^{2+} to Co^0 . As a result the nanostructured composite material in which Co nanoparticles are dispersed in the polymer matrix is formed. The reflection peaks of β -Co nanoparticles of a cubic face-centered lattice are identified in the diffraction pattern of the nanocomposite at scattering angles 2θ close to 68.35° , 80.65° (Figure 3).

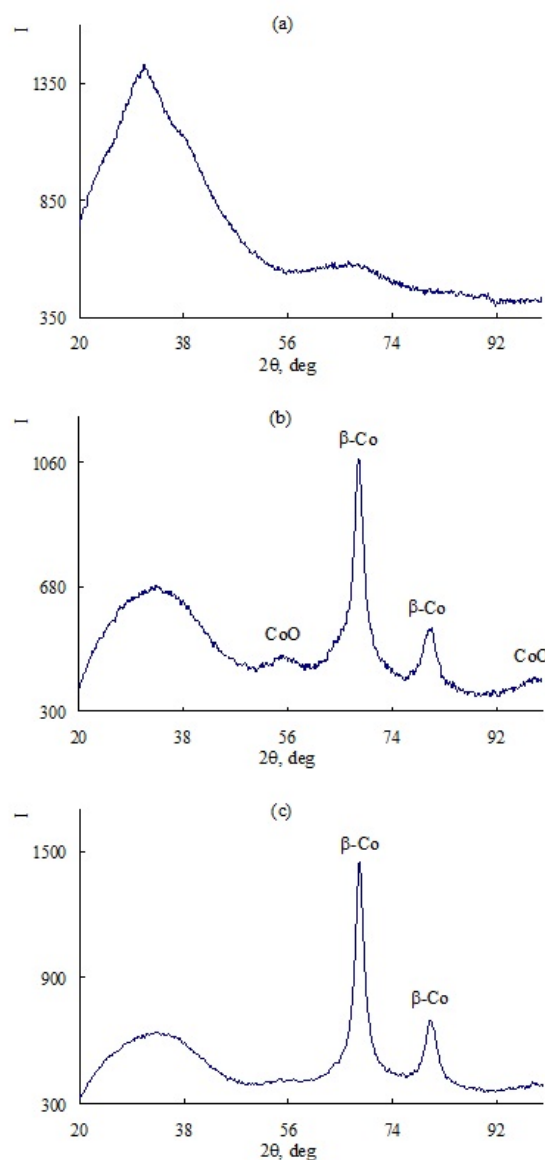


Figure 3. XRD patterns of PPOA (a) and Co/PPOA nanocomposite, obtained at $T = 450$ (b) and 500 °C (c) while heating for 10 min.

The Co crystallites size distribution determined by XRD analysis.²⁶ Figure 4 shows the size distribution of coherent scattering regions in Co nanoparticles.

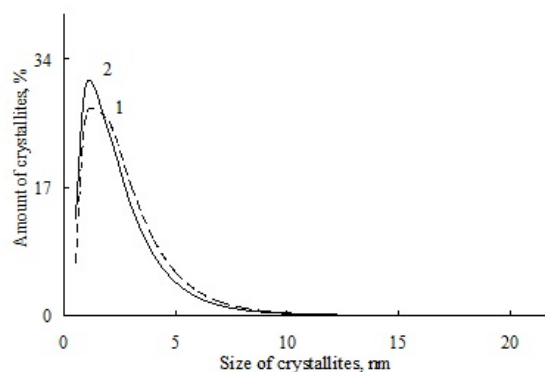


Figure 4. Distribution of crystallites by Co size in Co/PPOA nanocomposite, obtained at $T = 500$ (1) and 650 °C (2) while heating for 10 minutes.

Size distribution curves are narrow. About 90–95 % of Co crystallites have size less than 5 nm. Co/PPOA metal-polymer nanocomposite is a black powder, insoluble in organic solvents.

The influence of the synthesis conditions (temperature, heating time and Co concentration) on the yield of Co/PPOA nanocomposite was studied. It was found that the yield of the nanocomposite slightly decreases (4–6 %) with the increase of heating time and temperature (Figure 5).

A study of synthesis temperature effect on the Co/PPOA nanocomposite structure has shown that at $T < 500$ °C there are both the Co and CoO nanoparticles in the nanocomposite indicated by XRD peaks at scattering angles $2\theta = 55.61^\circ$, 65.32° , 99.05° (Figure 3b). The increase of heating time from 5 up to 30 minutes does not lead to the complete reduction of CoO to Co.

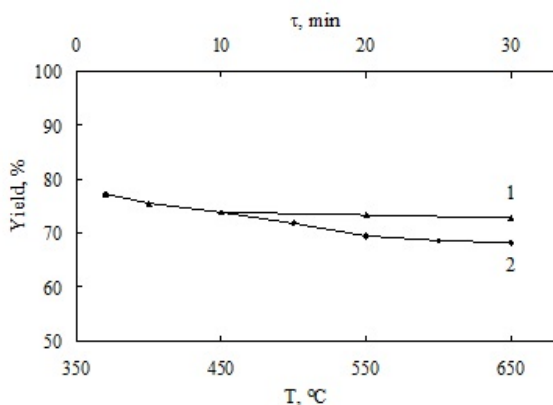


Figure 5. Dependence of the yield of Co/PPOA nanocomposite from the heating time (1) and the temperature (2). Nanocomposite was obtained at $T = 450$ °C (1) while heating for 10 min (2).

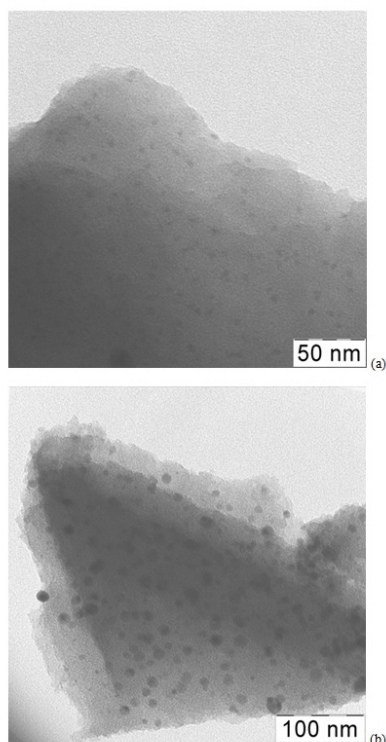


Figure 6. Microphotographs of Co/PPOA nanocomposite, obtained at $T = 500$ °C (a) and 650 °C (b) with $[Co] = 10$ wt. % at the loading.

In the inert atmosphere at the temperature range 500–650 °C and the duration of IR heating for 10 minutes, only metal Co nanoparticles are identified. According to AAS the content of cobalt in the nanocomposite obtained at 550 °C is 22.6 wt. %. Figure 6 shows the microphotographs of Co/PPOA nanocomposite. At the temperature of 500 °C Co nanoparticles of the spherical shape with the size of 4 nm are formed (Figure 6a). The increase of the synthesis temperature to 650 °C leads to the formation of nanoparticles with size $4 < d < 14$ nm.

An investigation of the Co concentration effect on the structure of the Co/PPOA nanocomposite has shown that at Co concentration $[Co] = 5$ –10 wt. % at $T = 500$ °C only reduced Co nanoparticles are identified on the XRD patterns of the nanocomposite. Co concentration increase to $[Co] = 15$ –30 wt. % leads to CoO nanoparticles amount increase and makes them dominant form of Co in the nanocomposite (Figure 7).

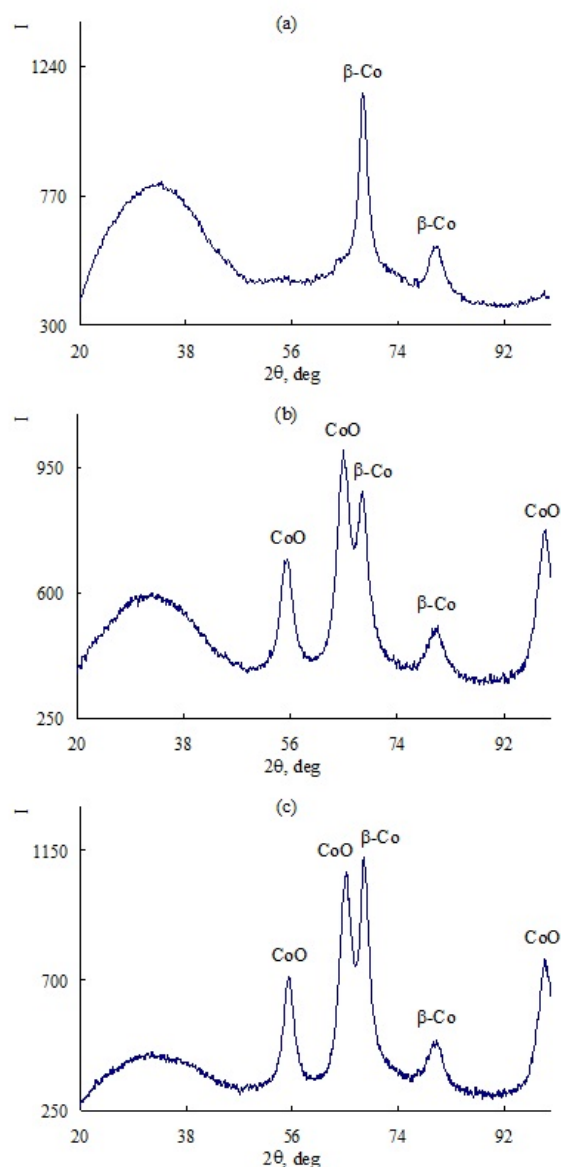


Figure 7. XRD patterns of Co/PPOA nanocomposite, obtained at $T = 500$ °C while heating for 10 min with the cobalt content at the loading equal to 5 (a), 15 (b) and 30 wt. % (c).

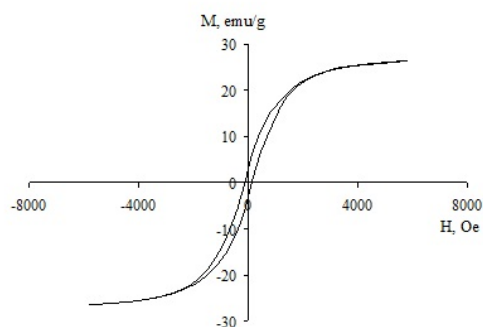


Figure 8. Magnetization of Co/PPOA nanocomposite, obtained at $T = 500\text{ }^{\circ}\text{C}$ while heating for 10 min as a function of the applied magnetic field at the room temperature.

An investigation of magnetic properties at room temperature showed that the obtained Co/PPOA nanomaterial has hysteresis magnetization reversal. The dependence of the magnetization on the applied magnetic field is shown in Figure 8. The values of the main magnetic characteristics were found: saturation magnetization $M_S = 26.4\text{ emu g}^{-1}$, coercive force $H_C = 134\text{ Oe}$, residual magnetization $M_R = 3.1\text{ emu g}^{-1}$. The squareness coefficient of the hysteresis loop k_S , which is the ratio of the residual magnetization M_R to the saturation magnetization M_S is 0.11. The obtained value $M_R/M_S = 0.11$ is characteristic of uniaxial, single-domain particles²⁷ and indicates of the superparamagnetic behavior of the nanocomposite.

The thermal stability of the Co/PPOA nanocomposite was studied by TGA and DSC. The temperature dependence of weight of the Co/PPOA nanocomposite compared to the PPOA after heating at $1000\text{ }^{\circ}\text{C}$ in the nitrogen flow and in the air is shown in Figure 9.

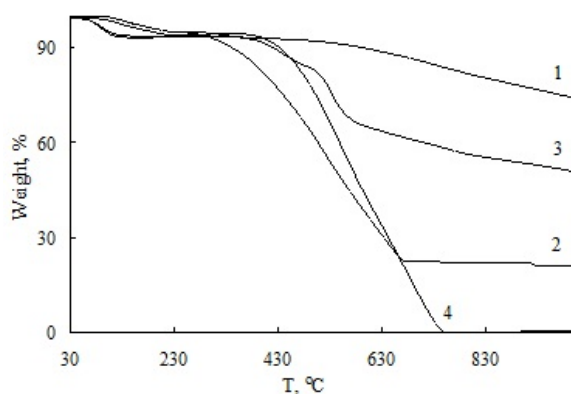


Figure 9. Weight dynamics of Co/PPOA nanocomposite (1, 2) and PPOA (3, 4) at heating to $1000\text{ }^{\circ}\text{C}$ at heating rate $10\text{ }^{\circ}\text{C min}^{-1}$ in nitrogen flow (1, 3) and in air (2, 4).

Co/PPOA nanocomposite is characterized by the high thermal stability. 7 % weight loss at $116\text{ }^{\circ}\text{C}$ occurs due to the presence of moisture in the nanocomposite, which is proved by DSC data (Figure 10). In the DSC thermogram of Co/PPOA nanocomposite there is an endothermic peak in this range of temperatures which is absent after reheating. After moisture removal the mass of the Co/PPOA nanocomposite does not change up to $300\text{ }^{\circ}\text{C}$. The absence

of weight loss in this temperature range is associated with the fact that during the nanocomposite synthesis the condensation reaction of phenoxazine oligomers proceeds and leads to the growth of the polymer chain. Opposite to the Co/PPOA nanocomposite in PPOA the weight loss at $230\text{ }^{\circ}\text{C}$ is observed and it is associated with the decomposition of low-molecular fraction contained in the polymer as proved by DSC data.²¹ There is an endothermic peak at $285\text{ }^{\circ}\text{C}$ on the DSC thermogram of PPOA which is associated with decomposition. The lack of the endothermic peak after reheating excludes melting at $285\text{ }^{\circ}\text{C}$. According to XRD analysis PPOA is an amorphous polymer (Figure 3a).

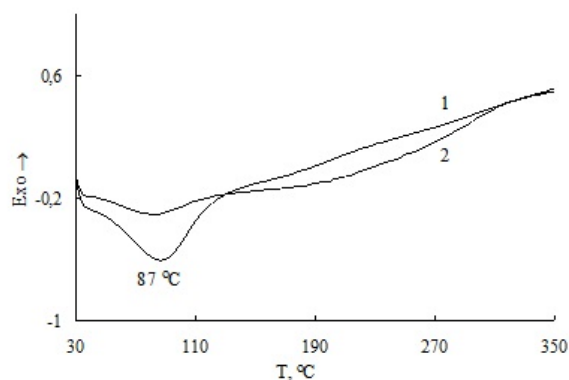


Figure 10. DSC thermograms of Co/PPOA nanocomposite at heating to $350\text{ }^{\circ}\text{C}$ in nitrogen flow at heating rate $10\text{ }^{\circ}\text{C min}^{-1}$ (1 – first heating, 2 – second heating).

In the inert atmosphere in Co/PPOA nanocomposite there is a gradual weight loss and at $1000\text{ }^{\circ}\text{C}$ the residue is 75 %. In PPOA at $1000\text{ }^{\circ}\text{C}$ the residue is 51 %. In the air the nanocomposite is less thermally stable than PPOA. The main processes of thermal-oxidative destruction in PPOA start at $430\text{ }^{\circ}\text{C}$ and in Co/PPOA nanocomposite at $330\text{ }^{\circ}\text{C}$. PPOA loses half of its initial weight at $580\text{ }^{\circ}\text{C}$ and the nanocomposite at $546\text{ }^{\circ}\text{C}$.

Conclusions

An investigation of thermal transformations of PPOA in the presence of cobalt(II) acetate under IR heating has shown that the nanostructured composite material based on PPOA and Co nanoparticles is formed. Magnetic particles have size $4 < d < 14\text{ nm}$ providing single-domain criteria. Squareness coefficient of the hysteresis loop $k_S = 0.11$, which indicates of a sufficient part of superparamagnetic particles of cobalt. It was shown that Co/PPOA nanocomposite has a high thermal stability. The residue at $1000\text{ }^{\circ}\text{C}$ in the inert atmosphere is 75 %.

Acknowledgements

The work has been supported in part by the Russian Foundation for Basic Research, project № 14-03-31556 mol_a.

Authors thank G.A. Shandryuk (TIPS RAS) for conducting the thermal analysis of the Co/polyphenoxazine nanocomposite.

References

- ¹Sellinger, A., Weiss, P. M., Nguyen, A., Lu, Y., Assink, R. A., Gong, W., Brinker, C. J., *Nature*, **1998**, *394*, 256.
- ²Yamamoto, K., Sakata, Y., Nohara, Y., Takahashi, Y., Tatsumi, T., *Science*, **2003**, *300*, 470.
- ³Gerasin, V. A., Antipov, E. M., Karbushev, V. V., Kulichikhin, V. G., Karpacheva, G. P., Talroze, R. V., Kudryavtsev, Y. V., *Russ. Chem. Rev.*, **2013**, *82*, 303.
- ⁴Pomogailo, A. D., Rozenberg, A. T., Uflyand, I. E., *Metal Nanoparticles in Polymers* (Khimiya, Moscow, **2000**, 672 p.) [in Russian].
- ⁵Yang, C., Du, J., Peng, Q., Qiao, R., Chen, W., Xu, C., Shuai, Z., Gao, M., *J. Phys. Chem. B*, **2009**, *113*, 5052.
- ⁶Aphesteguy, J. C., Jacobo, S. E., *Physica B*, **2004**, *354*, 224.
- ⁷Liu, W., Kumar, J., Tripathy, S., Senecal, K. J., Samuelson, L., *J. Am. Chem. Soc.*, **1999**, *121*, 71.
- ⁸Qiu, G., Wang, Q., Nie, M., *J. Appl. Polym. Sci.*, **2006**, *102*, 2107.
- ⁹Zhang, Z., Wan, M., *Synth. Met.*, **2003**, *132*, 205.
- ¹⁰Ding, X., Han, D., Wang, Z., Xu, X., Niu, L., Zhang, Q., *J. Colloid. Interface Sci.*, **2008**, *320*, 341.
- ¹¹Hsieh, T. H., Ho, K. S., Huang, C. H., Wang, T. Z., Chen, Z. L., *Synth. Met.*, **2006**, *156*, 1355.
- ¹²Reddy, K. R., Lee, K.-P., Iyengar, A. G., *J. Appl. Polym. Sci.*, **2007**, *104*, 4127.
- ¹³Reddy, K. R., Lee, K. P., Gopalan, A. I., *J. App. Polym. Sci.*, **2007**, *106*, 1181.
- ¹⁴Zhu, Y. G., Li, Z. Q., Gu, J. J., Zhang, D., Tanimoto, T., *J. Polym. Sci. B., Polym. Phys.*, **2006**, *44*, 3157.
- ¹⁵Morrish, A. H. *The physical principles of magnetism*. Wiley: New York. 1965, p. 344.
- ¹⁶Gubin, S. P., Koksharov, Yu. A., Khomutov, G. B., Yurkov, G. Yu., *Russ Chem. Rev.*, **2005**, *74*, 489.
- ¹⁷Chernavskii, P. A., Pankina, G. V., Lunin, V. V., *Russ. Chem. Rev.*, **2011**, *80*, 579.
- ¹⁸Karpacheva, G., Ozkan, S., *Procedia Mater. Sci.*, **2013**, *2*, 52.
- ¹⁹Ozkan, S. Zh., Dzidziguri, E. L., Chernavskii, P. A., Karpacheva, G. P., Efimov, M. N., Bondarenko, G. N., *Nanotechnologies in Russia*, **2013**, *8*, 452.
- ²⁰Ozkan, S. Zh., Karpacheva, G. P., in: *Handbook of Chemistry and Chemical Biology. Methodologies and Applications*, Ed. R. Joswik, A. A. Dalinkevich, Apple Academic Press Inc., USA-Canada, Toronto, New Jersey, **2014**, *5*, 53.
- ²¹Ozkan, S. Zh., Karpacheva, G. P., Bondarenko, G. N., *Rus. Chem. Bull.*, **2011**, *60*, 1651.
- ²²Zemtsov, L. M., Karpacheva, G. P., Efimov, M. N., Muratov, D. G., Bagdasarova, K. A., *Polym. Sci. B.*, **2006**, *48*, 633.
- ²³Chernavskii, P. A., Khodakov, A. Y., Pankina, G. V., Girardon, J.-S., Quinet, E., *Appl. Catal.*, **2006**, *306*, 108.
- ²⁴Ozkan, S. Zh., Kozlov, V. V., Karpacheva, G. P., *J. Balkan Tribological Association*, **2010**, *16*, 393.
- ²⁵Ozkan, S. Zh., Dzidziguri, E. L., Karpacheva, G. P., Bondarenko, G. N., *Nanotechnologies in Russia*, 2011, *6*, 750.
- ²⁶Dzidziguri, E. L., *Nanotechnologies in Russia*, 2009, *4*, 857.
- ²⁷Madsen, K. N., *J. Magn. Magn. Mater.*, **2002**, *241*, 220.

Received: 19.12.2014.

Accepted: 10.03.2015.